Correlation of metabolic characteristics with diffusion tensor imaging in human gliomas

G. A. Fellows[1], A. J. Wright[2], T. R. Barrick[3], D. J. McIntyre[4], C. A. Clark[5], B. A. Bell[6], and F. A. Howe[7]

[1]Department of Neurosurgery, King's College Hospital London NHS Trust, London, United Kingdom, [2]Radiology, UMC st. Radboud University Hospital, Nijmegen, Netherlands, [3]Clinical Neuroscience, St George's, University of London, London, United Kingdom, [4]CRUK Cambridge Research Institute, Cambridge, United Kingdom, [5]Radiology and Physics Unit, UCL Institute of Child Health, London, United Kingdom, [6]Academic Neurosurgery, St George's, University of London, London, United Kingdom, [7]Cardiac & Vascular Sciences, St George's, University of London, London, United Kingdom

Introduction: Gliomas are the most common primary brain tumour type in adults and because they are highly infiltrative, there is often difficulty in defining their boundaries to aid planning of surgical and radiation treatments. DTI provides median diffusivity (MD) and anisotropy (FA) for describing tissue structure and so provides a more subtle characterisation of tumour infiltration [1] and correlation to ^{1}H MRS than simple DWI [3-5]. Metabolite maps obtained by ^{1}H MRSI provide complementary information to DTI and independent component analysis of ^{1}H MRSI from glioma has been used to define regions related to tumour core, infiltration and normal brain that have specific DTI characteristics [2]. In this study we investigate the relationship between individual metabolites and DTI metrics to better understand the underlying tissue changes that drive the alterations in MD and FA in gliomas and the surrounding brain tissue.

Methods: ***Data acquisition*** 30 patients were studied prior to treatment whose subsequent histopathologically diagnosed tumour types were: 13 WHO grade II gliomas (8 grade II astrocytomas, 3 gemistocytic astrocytomas and 2 oligoastrocytomas), 5 grade III astrocytomas and 12 glioblastoma multiforme. MRI & MRS were performed at 1.5T and included: 2D MRSI with 16 by 16 phase encode steps over 22 cm FOV and 15 mm slice thickness at TE 30 ms & TR 2000 ms with PRESS localisation to the bulk of the tumour and surrounding tissue; DTI with 2.8 mm thick slices and 2.8 mm gap, with b =1000 s mm^{-2} and 12 gradient orientations; conventional T2-weighted and FLAIR images. ***Data reconstruction*** The raw MRSI data were zero-filled once in both spatial dimensions with metabolite quantification performed with LCModel. MRSI and DTI maps were co-registered and average FA and MD calculated for each spectroscopy voxel. For each patient, single lines of voxels from tumour core to normal white matter were selected based on the appearance on T2 or FLAIR images. ***Statistical analyses*** Linear regression analyses were made of individual metabolite concentrations (NAA, total Choline (tCho), total Creatine (tCr), myo-Inositol and lipids) against FA and MD for grade II and GBM tumour groups. *P* values for significance are given after scaling each original value with Holm's correction factor for multiple comparisons [6].

Results: Highly significant correlations were found for NAA and tCr with both FA and MD in grade II and GBM data groups (e.g. Figs 1 and 2 where each data point is for an individual voxel). The strongest correlations were for: FA *v.* NAA in both grade II and GBM ($R = 0.7$, $p < 0.005$). MD showed inverse correlation with tCr (grade II: $R = -0.5$, $p < 0.005$; GBM: $R = -0.34$, $p < 0.05$) and NAA (grade II: $R = -0.6$ $p < 0.005$). NAA was also strongly correlated with tCr (grade II: $R = 0.6$, $p < 0.005$; GBM: $R = 0.5$, $p < 0.005$), but not with tCho. There was no correlation of DTI with any other metabolites. Of particular note was that the plots of NAA *v.* FA intercepted at non-zero FA for voxel-line data in all tumour groups (Fig 2) as well as for full 2D MRSI data sets (Fig 3), although there was considerably more scatter in the latter.

Discussion: Variations in FA and MD within gliomas and the surrounding tissue are dependent on tissue structure (cell density, oedema and necrosis) and cell type (tumour or brain). The correlations of MD & FA with tCr & NAA indicate the loss of neuronal tissue and replacement with tumour or necrosis are the main driving factors in the change in DTI parameters in moving from normal white matter to tumour core. Although some previous studies have indicated an inverse correlation of tCho with MD due to dominating effects of tumour cell density [3-5], we do not see this over our datasets of different patients and glioma types. Increased tCho is frequently associated with increased cellular proliferation of tumours, but tumour metabolism is also highly variable, hence it may not be surprising that in general tCho does not correlate with MD. The strong correlation of NAA and FA supports the use of FA as a surrogate marker for viable neurones in infiltrative gliomas, with the advantage of the better spatial resolution of DTI over MRSI. The non-zero FA intercept in Figs 2 and 3 could indicate anisotropic structure within gliomas as reported in a recent study [7], and even after complete neuronal loss, could be due to the gliomas original growth pattern along neuronal tracts. Alternatively, because FA is calculated from principal diffusion magnitude images there is an artefactual "floor" of a minimum non-zero calculated FA arising from the noise. However, a theoretical analysis to simulate our data shows this minimum FA to be ≈0.05, much lower than the average intercept of 0.1.

In conclusion, in terms of determining objective markers of glioma infiltration, the correlation of MRS with DTI appears more strongly dependent on the loss of viable neurones rather than on the presence of tumour cells. Combination of DTI and MRS data may allow statistical analyses to provide objective measures of tumour boundaries from DTI data, but the presence of non-zero FA within gliomas must be included in the model.

Fig.1 Voxel line data for high-grade gliomas

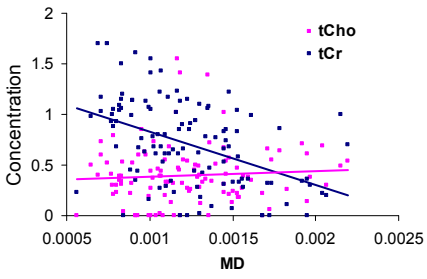

Fig. 2 Voxel line data for each tumour group

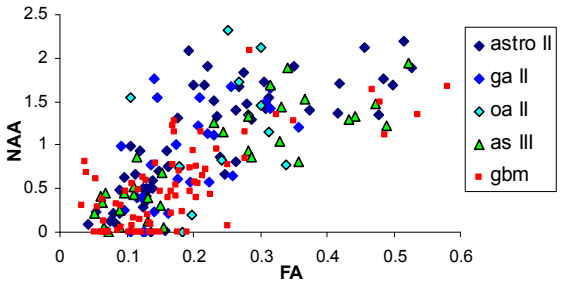

Fig 3. Scatter plot of GBM data

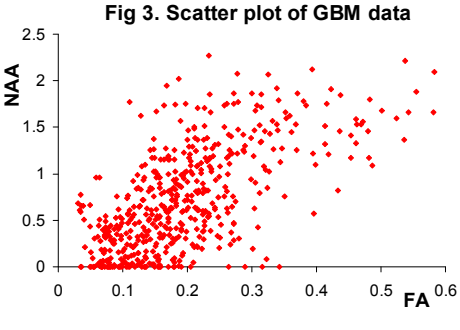

References [1] SJ Price et al. *Eur Radiol* **17**:1675-84;2007. [2] AJ Wright et al. *Magn Reson Med* Epub Sept 25;2009. [3] IS Khayal et al. *J Magn Reson Imag* **27**:718–725;2008. [4] RK Gupta et al. *Magn Reson Med* **41**:2–7;1999. [5] D Wagnerova et al. *Magn Reson Mater Phy* **22**:19–31;2009. [6] Holm S. *Scand J Stat*;**6**:65–70;1979. [7] IS Khayal et al. *NMR Biomed* **22**: 449–455;2009

Acknowledgements This work was funded by European Union Framework 6 project "eTUMOUR", grant number LSHC-CT-2004-503094 and Cancer Research UK, Grant number: C8807/A3870.